Environmental Science
Processes & Impacts

PAPER

View Article Online
View Journal | View Issue

Cite this: *Environ. Sci.: Processes Impacts*, 2014, **16**, 1282

Effects of the preparation method and humic-acid modification on the mobility and contaminant-mobilizing capability of fullerene nanoparticles (nC_{60})

Lilin Wang,[ab] Lei Hou,[a] Ximeng Wang[a] and Wei Chen*[a]

Colloidal fullerene nanoparticles (nC_{60}) in aquatic environments may significantly affect the transport and risks of hydrophobic organic contaminants by serving as a contaminant carrier. The objective of this study was to understand how the combined variables of the preparation method and natural organic matter modification of nC_{60} might affect the mobility and contaminant-mobilizing capability of nC_{60}, by affecting the physicochemical properties of nC_{60}. We found that an nC_{60} sample prepared by sonicating C_{60} powder in deionized water (son_nC_{60}) was much less mobile in saturated sandy soil columns than an nC_{60} sample prepared by solvent-exchanging from toluene to water (tol_nC_{60}), because son_nC_{60} was considerably larger in size. However, son_nC_{60} exhibited greater capability to bind 2,2′,5,5′-polychlorinated biphenyl (PCB), likely because its loosely packed structures rendered more pore spaces, which were favorable adsorption sites for PCB. Forming nC_{60} samples in Suwannee River humic acid (SRHA) solution (instead of deionized water) only moderately affected the mobility of nC_{60}, but had very significant effects on the contaminant-binding capability of nC_{60}, especially when nC_{60} was prepared using the solvent exchange method. Adding SRHA after the formation of nC_{60} had varied effects on the mobility and contaminant-binding capability of nC_{60}, but the fundamental mechanism seems to be linked to how and to what extent SRHA had affected the aggregation/packing of C_{60} monomers. An important environmental implication is that nC_{60} formed under different environmental conditions might have vastly different effects on contaminant transport and risks.

Received 31st October 2013
Accepted 23rd December 2013

DOI: 10.1039/c3em00577a

rsc.li/process-impacts

Environmental impact

Buckminsterfullerene (C_{60}) is an important engineered carbon nanomaterial with many promising applications. However, the increasing production and use of C_{60} will increase the likelihood of its environmental release. In an aqueous environment C_{60} can form colloidal nanoparticles (nC_{60}), which may significantly enhance the transport and risks of hydrophobic organic contaminants by serving as a contaminant carrier. This study demonstrates that the mobility and contaminant-mobilizing capability of nC_{60} are largely dependent on the specific formation routes of C_{60} aggregates under complex environmental conditions. The underlying mechanism is that these combined variables determine the aggregation properties of C_{60}, and consequently, the mobility of nC_{60} and the nature of nC_{60}–contaminant interactions.

1 Introduction

Buckminsterfullerene (C_{60}) is an important engineered carbon nanomaterial with many promising applications in the areas of materials science, biomedicine, and environmental technology.[1–3] The increasing production and use of C_{60}, however, will increase the likelihood of its environmental release.[4] Even though molecular C_{60} is extremely hydrophobic,[5] colloidal C_{60} nanoparticles (nC_{60}) can be formed through solvent exchange, sonication, or long-term mixing.[6–11] Colloidal nC_{60} can be highly stable in an aquatic environment and can migrate through soil and aquifer materials.[12–14] Moreover, it has been demonstrated that nC_{60} has strong adsorption affinities for highly hydrophobic organic contaminants such as polychlorinated biphenyls (PCBs) and polycyclic aromatic hydrocarbons (PAHs), and might significantly enhance the transport and risks of such contaminants.[15–17]

Studies have shown that nC_{60} formed by different methods—in particular, physical mixing *versus* solvent exchange—can exhibit significantly different physicochemical characteristics

[a]*College of Environmental Science and Engineering/Ministry of Education Key Laboratory of Pollution Processes and Environmental Criteria/Tianjin Key Laboratory of Environmental Remediation and Pollution Control, Nankai University, Wei Jin Road 94, Tianjin 300071, China. E-mail: chenwei@nankai.edu.cn; Fax: +86-22-66229516; Tel: +86-22-66229516*

[b]*Sichuan Key Laboratory of Agricultural Environmental Engineering/College of Resources and Environment, Sichuan Agricultural University, Chengdu, Sichuan 611130, China*

such as surface charge, particle size, and stability.[6,8,18,19] In general, nC_{60} samples obtained by extended mixing (in the absence of organic solvents) are typically of larger particle sizes and more irregularly shaped,[8,19] in comparison with nC_{60} samples prepared using the solvent exchange methods, which tend to have crystal-like structures and are smaller in size.[6,9,20] Such formation-method-induced differences in physicochemical properties likely will have marked effects on the mobility of nC_{60} (accordingly to Espinasse *et al.*,[12] even nC_{60} samples prepared by solvent exchange can exhibit significantly different mobility depending on the solvents used). Furthermore, owing to their large differences in physicochemical properties, nC_{60} samples prepared using different methods likely will exhibit remarkably different affinities for environmental contaminants, and consequently, may possess different contaminant-mobilizing capabilities; however, this has not been examined systematically.

When released into the aquatic environment C_{60} or nC_{60} will inevitably interact with natural organic matter (NOM), which is ubiquitous and abundant in aquatic environments. Such interactions can significantly affect the morphology and surface chemistry of nC_{60},[21–23] and consequently, the mobility[12,24,25] and contaminant-mobilizing capabilities[24] of nC_{60} in porous media. For example, Duncan *et al.*[8] reported that the average particle sizes of nC_{60} prepared by stirring C_{60} particles in NOM solutions were considerably smaller than those of an nC_{60} sample prepared in nanopure water (without NOM). Wang *et al.*[25] found that the mobility of nC_{60} in saturated quartz sand columns was considerably enhanced by the presence of humic/fulvic acids (20 mg C l^{-1}) in the influent. In our previous study we found that nC_{60} formed in an NOM solution had significantly greater contaminant-mobilizing capability than nC_{60} formed in deionized water.[24] Herein, we further hypothesize that the specific effects of NOM on the mobility and contaminant-mobilizing capability of nC_{60} likely will depend on the routes through which nC_{60} is formed (*e.g.*, physical mixing *vs.* solvent exchange) and on the modes in which C_{60} makes contact with NOM (*e.g.*, during or after the formation of nC_{60}).

The primary objective of this study was to understand how the mobility and contaminant-mobilizing capability of nC_{60} in saturated porous media respond to the combined variables of the preparation method and NOM modification. Six nC_{60} samples were prepared by two different methods, *i.e.*, sonication and solvent exchange. The effects of NOM on the physicochemical properties of nC_{60} were examined by introducing Suwannee River humic acid (SRHA) either during or after the formation of nC_{60}. The different nC_{60} samples were characterized for morphological and surface chemistry properties. Column tests were conducted to examine the transport properties of different nC_{60} samples in saturated sandy soil, and the capabilities of the nC_{60} samples to enhance the transport of 2,2′,5,5′-polychlorinated biphenyl (PCB). The correlations between the physicochemical properties of the nC_{60} samples and the mobility and contaminant-mobilizing capabilities of the nC_{60} samples are discussed.

2 Experimental

2.1 Materials

Sublimed fullerene powder (C_{60}, >99.5%) was purchased from SES Research (Houston, TX). SRHA was purchased from International Humic Substances Society (St. Paul, MN). PCB was purchased from Sigma-Aldrich (St. Louis, MO). Lula soil, containing 45% sand, 36% silt, and 19% clay, was collected from a ranch near Lula, OK. The fractional organic carbon (f_{OC}) value of the soil is 0.0037.

2.2 Preparation and characterization of nC_{60} samples

The nC_{60} samples were prepared using both a solvent exchange method and a physical mixing method. The solvent exchange method was similar to that reported by Andrievsky *et al.*[26] Briefly, 20 ml of C_{60} solution (1 mg ml^{-1} in toluene) was added to 200 ml of deionized water and was sonicated with a probe (Vibra-Cell VCX800, Sonics & Material Inc., Newtown, CT) at 100 W for 3 h in the dark to generate a yellow-colored nC_{60} suspension. The suspension was filtered with a 1 μm glass fiber filter followed by a 0.45 μm membrane filter (Millipore Co., Billerica, MA) to remove large C_{60} aggregates. The obtained nC_{60} sample is referred to as "tol_nC_{60}". For the physical mixing method, the mixture of 100 mg C_{60} powder and 200 ml deionized water was sonicated at 100 W using the sonication probe for 2 h. The suspension was filtered as mentioned above. This sample is referred to as "son_nC_{60}". For each preparation method two SRHA-modified samples were prepared, by replacing the 200 ml deionized water with a SRHA solution (the obtained samples are referred to as "tol_nC_{60}/SRHA" and "son_nC_{60}/SRHA", respectively), or by adding tol_nC_{60} or son_nC_{60} to a SRHA solution and magnetically stirring for 4 h in the dark[11,27] (the obtained samples are referred to as "tol_nC_{60}+SRHA" and "son_nC_{60}+SRHA", respectively). The obtained nC_{60} samples were kept in the dark at 4 °C and were stable during the period of this study.

The concentrations of C_{60} in the six nC_{60} samples were determined using an oxidation–toluene extraction procedure.[17] Particle size distribution, average hydrodynamic diameters (Z_{ave}), and ζ potentials of the nC_{60} samples were measured by dynamic light scattering (DLS) and electrophoretic mobility, using a ZetaPALS (Brookhaven Instruments, Holtsville, NY). Transmission electron microscopy (TEM) images were obtained with a JEOL-2010 transmission electron microscope (Peabody, MA) operated at 80 kV. The samples were prepared by air-drying a drop of nC_{60} sample onto a copper TEM grid (Electron Microscopy Sciences, Hatfield, PA). Selected properties of the nC_{60} samples are listed in Table 1.

2.3 Column experiments

Column experiments were conducted using previously developed protocols.[17] Briefly, soil was dry-packed into Omnifit borosilicate glass columns (10 cm × 0.66 cm, Bio-Chem Valve Inc., Boonton, NJ) with 10 μm stainless-steel screens (Valco Instruments Inc., Houston, TX) on both ends. Each column contained approximately 3.2 g soil with an average length of

Table 1 Average hydrodynamic diameter (Z_{ave}) and ζ potential values of different nC_{60} samples

Sample ID	Z_{ave} (nm)	ζ Potential (mV)
son_nC_{60}	372.9	−23.87
son_nC_{60}/SRHA	309.4	−28.47
son_nC_{60}+SRHA	316.5	−25.37
tol_nC_{60}	164.9	−23.29
tol_nC_{60}/SRHA	124.5	−22.40
tol_nC_{60}+SRHA	151.4	−23.39

7.0 cm. The packed columns were first flushed with 60 ml of deionized water at a flow rate of 3 ml h^{-1} and then with 180 ml of 0.5 mM NaCl to stabilize the soil colloids. The porosity and dead volume were determined using tracer tests.

To prepare the influents, aliquots of the nC_{60} samples were diluted in electrolyte in amber glass vials to give an nC_{60} concentration of 5–6 mg l^{-1} in 0.5 mM NaCl. Then, a PCB solution in methanol was added with a micro-syringe to give a total PCB concentration of ~11 μg l^{-1} in each vial. The volume percentage of methanol was kept below 0.1% to minimize potential cosolvent effects. The vials were sealed with Teflon-lined screw caps and tumbled end-over-end at 3 rpm for 7 days.[17] Afterward, 2 ml of the suspension in each vial was taken to measure the nC_{60} concentration and the total PCB concentration. Another 4 ml of the suspension was passed through a 0.02 μm Al_2O_3 membrane (GE Whatman Corp., UK) to remove nC_{60}. The filtrate was collected and the concentration of dissolved PCB was analyzed.[17] The mass of PCB adsorbed to nC_{60} was calculated based on a mass balance.

The protocols of the column experiments are summarized in Table 2. In a typical column experiment, the influent was loaded to the soil column with a syringe pump.[24] The effluent was collected at predetermined time intervals, and the concentrations of both nC_{60} and PCB were measured (see *Analytical methods*).

2.4 Analytical methods

The concentrations of nC_{60} in the effluents were determined with a UV/vis spectrophotometer (UV-2401, Shimadzu Scientific Instruments, Columbia, MD),[24] and the detection limit was 0.02 mg l^{-1}. The presence of a small amount of SRHA in the solution had negligible effects on the C_{60} measurement (confirmed using the oxidation–toluene extraction procedure[17]). PCB in the effluents was extracted with hexane and the extraction efficiencies were 95 ± 3.5%. PCB in hexane was analyzed with a gas chromatograph (GC6890N, Agilent Corp., Santa Clara, CA) equipped with an electron capture detector. The detection limit was 0.05 μg l^{-1}.

3 Results and discussion

3.1 Characteristics of different nC_{60} samples

The particle size distribution data of the six nC_{60} samples are compared in Fig. 1, and the Z_{ave} values are summarized in Table 1. Two general observations can be made. First, the nC_{60} samples prepared using the physical mixing approach (sonication in the absence of organic solvents) are considerably larger in size compared with the nC_{60} samples prepared using the solvent exchange approach (this can be further understood with the TEM images shown in Fig. 2). The Z_{ave} values of the three nC_{60} samples prepared by sonication range from 309.4 to 372.9 nm, whereas the Z_{ave} values of the three nC_{60} samples prepared by solvent exchange are only from 124.5 to 164.9 nm. The difference appears to be attributable to whether nC_{60} was

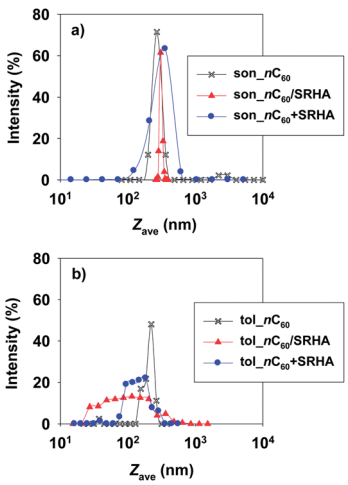

Fig. 1 Intensity-weighted particle size distribution of nC_{60} samples.

Table 2 Protocols and breakthrough results of nC_{60} and PCB of column experiments

	Column properties		Influent properties					Effluent properties[d]	
Exp. no.	θ^a	v^b (m d^{-1})	C_PCB (μg l^{-1})	Type of nC_{60}	C_nC_{60} (mg l^{-1})	C_SRHA (mg l^{-1})	Adsorbed mass[c] (%)	C/C_0_nC_{60} (%)	C/C_0_PCB (%)
1	0.46	9.9	10.7	son_nC_{60}	5.2	—	82	23.7 ± 0.9	10.6 ± 0.2
2	0.47	9.8	10.6	son_nC_{60}/SRHA	5.8	18.5	95	50.0 ± 0.6	25.8 ± 0.4
3	0.47	9.9	10.3	son_nC_{60}+SRHA	4.8	20	83	82.3 ± 2.4	57.9 ± 0.8
4	0.47	10.0	10.5	tol_nC_{60}	6.3	—	93	83.1 ± 0.3	21.3 ± 0.2
5	0.47	9.8	12.9	tol_nC_{60}/SRHA	5.5	8.4	95	92.1 ± 0.8	78.0 ± 2.1
6	0.47	9.7	12.6	tol_nC_{60}+SRHA	6.2	20.3	84	96.4 ± 1.1	17.7 ± 1.1

[a] Porosity of soil column. [b] Linear velocity. [c] Mass fraction of nC_{60}-adsorbed PCB in the influent. [d] Average value of the last three data points of the respective breakthrough curve.

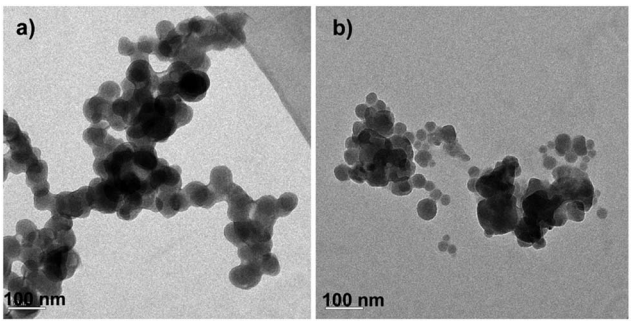

Fig. 2 Typical TEM images of son_nC$_{60}$ (a) and tol_nC$_{60}$ (b).

formed in a "top-down" fashion or a "bottom-up" fashion,[28] – the sonication approach is predominantly a "top-down" process (*i.e.*, large aggregates are broken into nano-sized smaller ones) whereas the solvent exchange approach is a "bottom-up" process (*i.e.*, colloidal aggregates are formed from monomer C$_{60}$ or crystal-like primary aggregates).[6,29] Second, SRHA modification appeared to have different effects on the samples prepared using the two different methods. Notably, for the two samples prepared by sonication (son_nC$_{60}$/SRHA and son_nC$_{60}$+SRHA) modification with SRHA resulted in significant reduction in particle size, however, for the two samples prepared by solvent exchange (tol_nC$_{60}$/SRHA and tol_nC$_{60}$+SRHA) significant reduction in particle size was only observed when SRHA was present during the formation of nC$_{60}$ (*i.e.*, tol_nC$_{60}$/SRHA) but not when SRHA was added after the formation of nC$_{60}$ (*i.e.*, son_nC$_{60}$+SRHA) (see Section 3.4 for detailed discussion on mechanisms). The two nC$_{60}$ samples prepared using different preparation methods in the absence of SRHA (son_nC$_{60}$ and tol_nC$_{60}$) had similar ζ potential values (Table 1). For both preparation methods modification with SRHA (either during or after the formation of nC$_{60}$) had very small effects on the ζ potential; this is consistent with the findings in the literature.[18,30,31]

3.2 Mobility of different nC$_{60}$ samples

The breakthrough data of different nC$_{60}$ samples are compared in Table 2 and Fig. 3, and two general observations can be made. First, the nC$_{60}$ samples prepared using the physical mixing method exhibited remarkably different mobility than the nC$_{60}$ samples prepared using the solvent exchange method. Second, the specific effects of SRHA modification on the mobility of the nC$_{60}$ samples were dependent on both the preparation method of nC$_{60}$ and the timing of SRHA addition.

Fig. 3a and c show that the breakthrough curves (BTCs) of son_nC$_{60}$ and tol_nC$_{60}$ are markedly different. For son_nC$_{60}$ the C/C_0 value (*i.e.*, the ratio of C$_{60}$ concentration in the effluent to the concentration in the influent) increased to a maximum value of 47% within 1–2 pore volume (PV) and then gradually declined to approximately 27% after 25 PV. The declination of the C$_{60}$ concentration in the effluent in the very early stage of the column experiment was likely caused by straining (*i.e.*, retention of particles at bounding surfaces or pore constrictions of the packed porous materials[14]). In comparison, the transport of tol_nC$_{60}$ reached a much larger C/C_0 value of 82% after 15 PV, even though the initial climbing of the C/C_0 value was slower. The much greater mobility of tol_nC$_{60}$ than son_nC$_{60}$ is likely because tol_nC$_{60}$ is much smaller in size (see the Z_{ave} value in Table 1 and the TEM images in Fig. 2) and possibly because it is more regularly shaped.

In Fig. 3a the BTCs of son_nC$_{60}$/SRHA and son_nC$_{60}$+SRHA are compared with that of son_nC$_{60}$. It is noteworthy that the BTCs of the two SRHA-modified nC$_{60}$ samples are markedly different; furthermore, each of the two BTCs is distinctively different from the BTC of the unmodified son_nC$_{60}$. The largest effect of SRHA modification was observed for son_nC$_{60}$+SRHA (*i.e.*, SRHA was added after nC$_{60}$ was formed), in that essentially 100% breakthrough was observed after 2–3 PV. Interestingly, once reaching its maximum the C/C_0 value started to decrease, and the BTC of son_nC$_{60}$+SRHA is essentially parallel to the BTC of son_nC$_{60}$. Adsorption of SRHA to nC$_{60}$ and to the surface of porous materials could enhance the steric repulsion between nC$_{60}$ and porous materials, and thus, inhibiting the deposition of nC$_{60}$.[32,33] However, because the size of son_nC$_{60}$+SRHA was still quite large (Table 1), straining was still in effect and resulted in the declination of C/C_0 after a few PV of the influent was injected into the column. The much smaller effect of SRHA observed on son_nC$_{60}$/SRHA was possibly because a considerable fraction of SRHA was incorporated into the C$_{60}$ aggregates, instead of coating on the surfaces of nC$_{60}$, because nC$_{60}$ was formed in the SRHA solution.

In Fig. 3c the BTCs of tol_nC$_{60}$/SRHA and tol_nC$_{60}$+SRHA are compared with that of tol_nC$_{60}$. In contrast to the vastly greater mobility of son_nC$_{60}$+SRHA than its non-modified counterpart (son_nC$_{60}$), only slightly enhanced mobility (mainly after 10 PV) was observed for tol_nC$_{60}$+SRHA, compared with tol_nC$_{60}$. This was likely because the mobility of tol_nC$_{60}$ was already quite significant. Nonetheless, tol_nC$_{60}$/SRHA exhibited considerably greater mobility than both tol_nC$_{60}$ and tol_nC$_{60}$+SRHA. This can probably be explained by the unique particle size distribution pattern of this nC$_{60}$ sample (Fig. 1b), in that it is characterized with a much wider peak, indicating that a significant fraction of C$_{60}$ aggregates was of small sizes. The initial faster climbing of the C/C_0 value for tol_nC$_{60}$/SRHA was likely related to the breakthrough of the smaller C$_{60}$ aggregates. Overall, it can be concluded (from the data in Fig. 3a and c) that even though modification with SRHA resulted in enhanced nC$_{60}$ mobility in general, the extent of the effects was highly dependent both on the specific preparation method *via* which nC$_{60}$ was formed and on the timing of SRHA addition.

3.3 Contaminant-mobilizing capabilities of different nC$_{60}$ samples

The BTCs of PCB in different column experiments are shown in Fig. 3b and d. In our previous study,[17] we demonstrated that under the experimental conditions such as those used in this study, no breakthrough of PCB would occur in the absence of nC$_{60}$ (and SRHA alone, at the concentrations similar to those in Table 2, could not result in any breakthrough of PCB). Thus, all

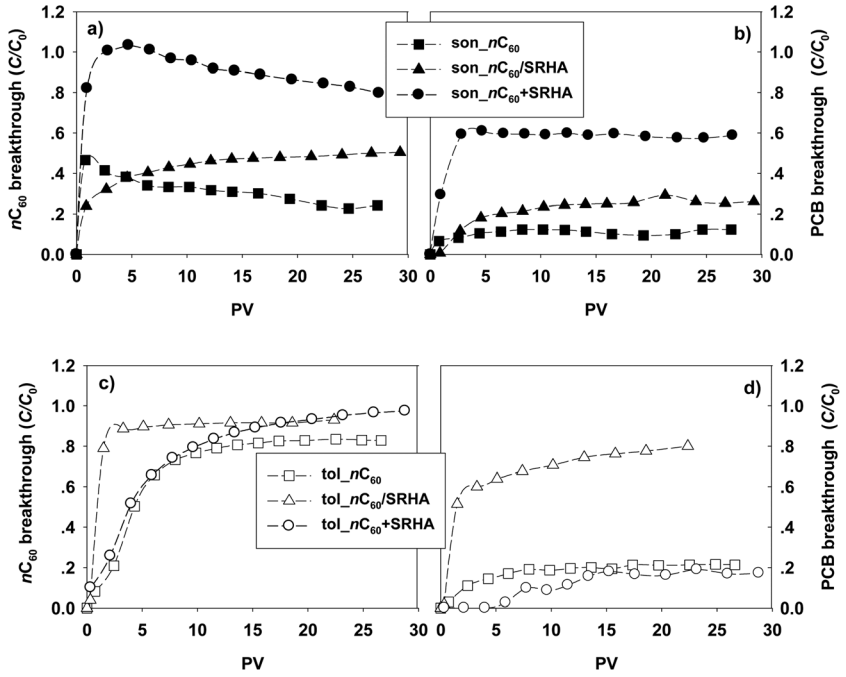

Fig. 3 Comparison of mobility and contaminant-mobilizing capability of different nC$_{60}$ samples. The left-hand-side plots show the breakthrough curves of different nC$_{60}$ samples in exp. 1–6 (Table 2), and the right-hand-side plots show the breakthrough curves of PCB in each of the experiments in the presence of different nC$_{60}$ carriers. PV = pore volume.

the PCB detected in the effluents of experiments 1–6 (Table 2) had to be that co-eluted with nC$_{60}$. Accordingly, the large differences in the C/C_0 values of PCB shown in Fig. 3b and d (the maximum breakthrough of PCB ranged from 11% for son_nC$_{60}$ to 78% for tol_nC$_{60}$/SRHA) indicate that the six different nC$_{60}$ samples had significantly different contaminant-mobilizing capabilities.

Note that the contaminant-mobilizing capabilities of nanoparticles depend on both the mobility of the nanoparticles and the adsorptive affinities of the nanoparticles for the contaminant molecules being mobilized.[16,34] Given the large differences in mobility among the six different nC$_{60}$ samples, it is reasonable to assume that the large differences in contaminant-mobilizing capabilities among the nC$_{60}$ samples stemmed largely from their different mobility. However, a closer look at Fig. 3 indicates that mobility is by no means the only factor contributing to the largely differed contaminant-mobilizing capabilities among the nC$_{60}$ samples. For example, Fig. 3c shows that the maximum breakthrough of the three nC$_{60}$ samples prepared by solvent exchange all reached over 80% after 15 PV, however, the respective C/C_0 values of PCB (Fig. 3d) do not corroborate with the similarity in the mobility of nC$_{60}$ at all. Thus, the results clearly indicate that the six nC$_{60}$ samples likely also differ significantly in adsorption affinities for PCB.

To better understand the differences among the six nC$_{60}$ samples in affinities for PCB, a contaminant-binding capability index, I, is defined as follows:

$$I = \frac{m_{\mathrm{PCB\_out}}}{m_{\mathrm{PCB\_out\_max}}} \quad (1)$$

where $m_{\mathrm{PCB\_out}}$ is the mass of PCB recovered in the effluent per unit PV, and $m_{\mathrm{PCB\_out\_max}}$ is the theoretically maximum mass of PCB that can be recovered in the effluent. The total mass of PCB contained in a unit PV of the influent ($m_{\mathrm{PCB\_0}}$) consists of two fractions, including the mass of dissolved PCB ($m_{\mathrm{PCB\_aq}}$) and the mass of PCB adsorbed to nC$_{60}$ ($m_{\mathrm{PCB\_ads}}$). Note that under the experimental conditions only nC$_{60}$-adsorbed PCB has the chance to break through the column. Thus, $m_{\mathrm{PCB\_out\_max}}$ can be derived as:

$$\begin{aligned} m_{\mathrm{PCB\_out\_max}} &= m_{\mathrm{PCB\_ads}} \cdot (C/C_0)_{n\mathrm{C}_{60}} \\ &= (m_{\mathrm{PCB\_0}} \cdot \mathrm{ads\%})(C/C_0)_{n\mathrm{C}_{60}} \end{aligned} \quad (2)$$

where ads% is the mass fraction of nC$_{60}$-adsorbed PCB in the influent and $(C/C_0)_{n\mathrm{C}_{60}}$ is the mass fraction of nC$_{60}$ breaking through the column (*i.e.*, the ratio of nC$_{60}$ concentration in the effluent to the concentration in the influent). Combining eqn (1) and (2) gives:

$$I = \frac{m_{\mathrm{PCB\_out}}}{(m_{\mathrm{PCB\_0}} \cdot \mathrm{ads\%})(C/C_0)_{n\mathrm{C}_{60}}} \quad (3)$$

or

$$I = \frac{\left(\frac{C}{C_0}\right)_{\mathrm{PCB}}}{\mathrm{ads\%}\left(\frac{C}{C_0}\right)_{n\mathrm{C}_{60}}} \quad (4)$$

where $(C/C_0)_{\mathrm{PCB}}$ is the ratio of PCB concentration in the effluent to the total PCB concentration in the influent. Note that when nC$_{60}$ flows through the soil column, the adsorbed PCB can partition out of nC$_{60}$ and sorbs to the sandy soil. Thus, the larger

the I value, the greater the contaminant-binding capability of nC$_{60}$. If the binding of PCB to nC$_{60}$ is completely irreversible, then the I value would be equal to 1 (the maximum possible value).

In Fig. 4 the I values of different nC$_{60}$ samples calculated using eqn (4) are compared. The plot shows the relative capability of different nC$_{60}$ samples to withhold the PCB molecules adsorbed to them. Therefore, the vast differences in the I values, as shown in Fig. 4, indicate that the specific preparation methods and the timing of SRHA modification greatly affected how the nC$_{60}$ samples could bind PCB.

3.4 Mechanistic aspects on contaminant-binding capabilities of nC$_{60}$ samples

Two general trends on the effects of the preparation method and SRHA modification on the contaminant-binding capabilities of nC$_{60}$ can be observed from Fig. 4. The first trend is that the non-modified nC$_{60}$ sample prepared by sonication (son_nC$_{60}$) has greater contaminant-binding capability than the non-modified nC$_{60}$ sample prepared by solvent exchange (tol_nC$_{60}$). The difference is likely linked to the morphological differences between the two samples. The formation routes of the two samples are completely reversed – for son_nC$_{60}$ the formation of C$_{60}$ aggregates is predominantly a "top-down" process,[28] in which large chunks of aggregates are broken into smaller ones by physical forces; for tol_nC$_{60}$, however, the formation of C$_{60}$ aggregates is a "bottom-up" process,[9,28] in which C$_{60}$ monomers first form highly ordered crystal-like primary aggregates and the primary aggregates further form larger secondary aggregates.[6,7,35] Consequently, son_nC$_{60}$ was more loosely packed and likely contained a greater amount of pore spaces with more tortuous pore geometry. Such unique morphological characteristics allowed son_nC$_{60}$ to bind contaminant molecules more strongly (pore spaces are energetically more favorable adsorption sites and can result in irreversible adsorption[36,37]). Additionally, the more loosely packed son_nC$_{60}$ was prone to structural rearrangements, which can further enhance the irreversible adsorption of adsorbed contaminant molecules,[36] by forming new pore spaces and thus entrapping contaminant molecules originally adsorbed on the surfaces of nC$_{60}$. A conceptual model is depicted in Fig. 5.

The second (and more striking) trend in Fig. 4 is that SRHA modification had markedly different effects on the contaminant-binding capabilities of nC$_{60}$ samples prepared using different methods. For the nC$_{60}$ samples prepared by physical mixing, SRHA modification enhanced contaminant-binding capabilities consistently (as indicated by the greater I values associated with son_nC$_{60}$/SRHA and son_nC$_{60}$+SRHA), even though different extents of enhancement were observed between the two SRHA-modified nC$_{60}$ samples. However, for the nC$_{60}$ samples prepared by solvent exchange, SRHA modification resulted in vastly enhanced contaminant-binding capability for one nC$_{60}$ sample (tol_nC$_{60}$/SRHA) but slightly inhibited contaminant-binding capability for the other sample (tol_nC$_{60}$+SRHA). The remarkably different effects of SRHA modification observed in this study again were related to the detailed routes *via* which nC$_{60}$ aggregates were formed.

As discussed earlier, when C$_{60}$ aggregates are formed by the solvent exchange method (*i.e.*, tol_nC$_{60}$), the aggregates are built from individual C$_{60}$ monomers. Because molecular C$_{60}$ is extremely hydrophobic, in aqueous solutions C$_{60}$ monomers are packed in a very tight fashion to minimize the surface areas exposed to water. However, when C$_{60}$ aggregates are formed in SRHA solution (as in the case of tol_nC$_{60}$/SRHA), SRHA (which possesses both hydrophilic and hydrophobic moieties) can

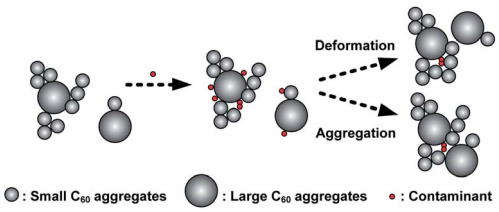

Fig. 5 Conceptual model showing irreversible adsorption of PCB molecules due to the physical rearrangements of C$_{60}$ aggregates for son_nC$_{60}$.

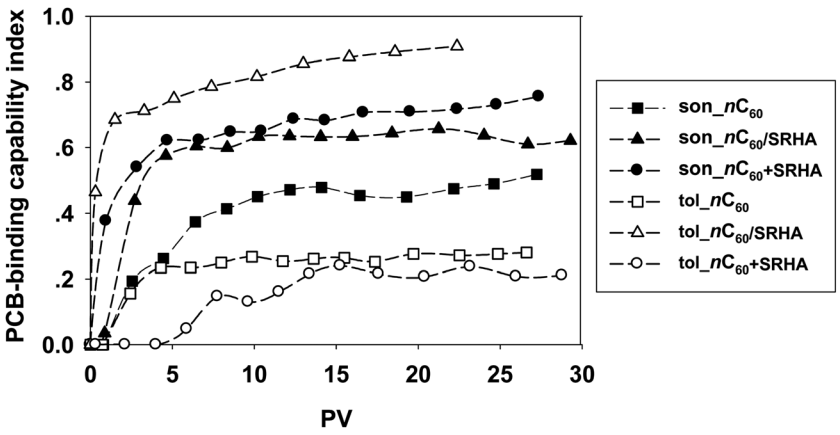

Fig. 4 Comparison of the PCB-binding capability of different nC$_{60}$ samples. The PCB-binding capability index was calculated using eqn (4). PV = pore volume.

serve as a dispersing agent,[11,30] which not only facilitates the phase transfer process, but more importantly, can result in the intercalation of SRHA within the C_{60} aggregates, likely making the aggregates less tightly packed and more porous owing to the steric hindrance effect of SRHA. This altered morphology of C_{60} aggregates would favor the binding of PCB molecules. Nonetheless, when SRHA is added after the C_{60} aggregates are formed (as in the case of tol_$n$$C_{60}$+SRHA), the abovementioned effects of SRHA are much less effective (or even largely diminished). It is possible that the addition of SRHA can break some of the secondary aggregates of $n$$C_{60}$, which seems to be a reasonable hypothesis based on Fig. 1b (wherein the particle size distribution of tol_$n$$C_{60}$+SRHA indicates the existence of aggregates with smaller sizes, compared with the non-modified tol_$n$$C_{60}$) and is consistent with the observations in previous studies.[11,30] However, it is unlikely that SRHA can significantly affect the pore structures of the aggregates. For tol_$n$$C_{60}$+SRHA the more predominant effect of SRHA is probably that the coating of SRHA on the surfaces of C_{60} aggregates blocks the pores of the aggregates, resulting in inhibited binding of contaminants.

Contrary to the "bottom-up" solvent exchange methods, the "top-down" physical mixing methods effect by breaking apart large chucks of aggregates into smaller ones by physical forces. Thus, even when this breaking-apart process occurs in a SRHA solution (as in the case of son_$n$$C_{60}$/SRHA), SRHA would not have the chance of making intimate interactions with monomer C_{60} (as in the case of tol_$n$$C_{60}$/SRHA), and the effects of SRHA modification on the morphology of C_{60} aggregates would be much smaller for son_$n$$C_{60}$/SRHA than for tol_$n$$C_{60}$/SRHA. Furthermore, because C_{60} aggregates formed by the physical mixing process are less ordered and more loosely packed, adding SRHA afterward can still result in significant further breaking of the relatively loosely packed C_{60} aggregates (which is consistent with the considerably smaller sizes of son_$n$$C_{60}$+SRHA than son_$n$$C_{60}$; see Table 1) and/or physical rearrangement of C_{60} aggregates (Fig. 5), and this explains the greater contaminant-binding capability of son_$n$$C_{60}$+SRHA than son_$n$$C_{60}$.

4 Conclusions

The specific routes through which $n$$C_{60}$ aggregates are formed can significantly affect the physicochemical properties of $n$$C_{60}$, and consequently, the mobility and contaminant-mobilizing capabilities of $n$$C_{60}$. The $n$$C_{60}$ samples formed *via* the "top-down" routes (*e.g.*, through extensive physical mixing or sonication of C_{60} powder in aqueous solutions in the absence of organic solvents) tend to be loosely packed and of greater amount of pores with tortuous geometry, whereas $n$$C_{60}$ samples formed *via* the "bottom-up" routes (*e.g.*, through solvent exchange) tend to be tightly packed and of ordered structures and smaller amount of pores. The presence of dissolved organic matters can significantly affect the size and morphology of C_{60} aggregates; however, the specific effects are largely dependent on the formation routes of $n$$C_{60}$. The abovementioned effects of formation routes and dissolved organic matters affect the mobility and contaminant-binding capability of $n$$C_{60}$ in a rather complicated manner. Nonetheless, the fundamental mechanism controlling the coupled effects of formation routes and dissolved organic matters seems to be linked to how they affect the aggregation/packing of C_{60} monomers, which in turn determine the size and morphology of $n$$C_{60}$ and how $n$$C_{60}$ can interact with environmental contaminants on the molecular level. While the abovementioned mechanisms remain to be verified with future studies that give more direct and microscopic evidence on the aggregation properties of $n$$C_{60}$ (particularly, characteristics of pore structures), one can conclude for now that $n$$C_{60}$ formed in natural aquatic environments can be of highly complex nature and can exert vastly different effects on contaminant transport and risks.

Acknowledgements

This project was supported by the Ministry of Science and Technology (Grant 2014CB932001), National Natural Science Foundation of China (Grants 21237002, 21177063, and 21307085), and China–U.S. Center for Environmental Remediation and Sustainable Development.

References

1 M. Campoy-Quiles, T. Ferenczi, T. Agostinelli, P. G. Etchegoin, Y. Kim, T. D. Anthopoulos, P. N. Stavrinou, D. D. C. Bradley and J. Nelson, *Nat. Mater.*, 2008, **7**, 158–164.
2 F. Simon, H. Peterlik, R. Pfeiffer, J. Bernardi and H. Kuzmany, *Chem. Phys. Lett.*, 2007, **445**, 288–292.
3 M. S. Mauter and M. Elimelech, *Environ. Sci. Technol.*, 2008, **42**, 5843–5859.
4 C. O. Hendren, X. Mesnard, J. Dröge and M. R. Wiesner, *Environ. Sci. Technol.*, 2011, **45**, 2562–2569.
5 J. Labille, A. Masion, F. Ziarelli, J. Rose, J. Brant, F. Villieras, M. Pelletier, D. Borschneck, M. R. Wiesner and J. Y. Bottero, *Langmuir*, 2009, **25**, 11232–11235.
6 J. A. Brant, J. Labille, J. Y. Bottero and M. R. Wiesner, *Langmuir*, 2006, **22**, 3878–3885.
7 K. L. Chen and M. Elimelech, *Langmuir*, 2006, **22**, 10994–11001.
8 L. K. Duncan, J. R. Jinschek and P. J. Vikesland, *Environ. Sci. Technol.*, 2008, **42**, 173–178.
9 J. D. Fortner, D. Y. Lyon, C. M. Sayes, A. M. Boyd, J. C. Falkner, E. M. Hotze, L. B. Alemany, Y. J. Tao, W. Guo, K. D. Ausman, V. L. Colvin and J. B. Hughes, *Environ. Sci. Technol.*, 2005, **39**, 4307–4316.
10 J. Lee and J.-H. Kim, *Environ. Sci. Technol.*, 2008, **42**, 1552–1557.
11 B. Xie, Z. Xu, W. Guo and Q. Li, *Environ. Sci. Technol.*, 2008, **42**, 2853–2859.
12 B. Espinasse, E. M. Hotze and M. R. Wiesner, *Environ. Sci. Technol.*, 2007, **41**, 7396–7402.
13 Y. Wang, Y. Li, J. D. Fortner, J. B. Hughes, L. M. Abriola and K. D. Pennell, *Environ. Sci. Technol.*, 2008, **42**, 3588–3594.
14 L. Zhang, L. Hou, L. Wang, A. T. Kan, W. Chen and M. B. Tomson, *Environ. Sci. Technol.*, 2012, **46**, 7230–7238.

15 X. K. Cheng, A. T. Kan and M. B. Tomson, *J. Mater. Res.*, 2005, **20**, 3244–3254.
16 T. Hofmann and F. von der Kammer, *Environ. Pollut.*, 2009, **157**, 1117–1126.
17 L. Zhang, L. Wang, P. Zhang, A. T. Kan, W. Chen and M. B. Tomson, *Environ. Sci. Technol.*, 2011, **45**, 1341–1348.
18 W. Zhang, U. S. Rattanaudompol, H. Li and D. Bouchard, *Water Res.*, 2013, **47**, 1793–1802.
19 X. Chang and P. J. Vikesland, *Environ. Pollut.*, 2009, **157**, 1072–1080.
20 J. Brant, H. Lecoanet and M. Wiesner, *J. Nanopart. Res.*, 2005, **7**, 545–553.
21 Q. Li, B. Xie, Y. S. Hwang and Y. Xu, *Environ. Sci. Technol.*, 2009, **43**, 3574–3579.
22 X. Qu, Y. S. Hwang, P. J. Alvarez, D. Bouchard and Q. Li, *Environ. Sci. Technol.*, 2010, **44**, 7821–7826.
23 M. Terashima and S. Nagao, *Chem. Lett.*, 2007, **36**, 302–303.
24 L. Wang, Y. Huang, A. T. Kan, M. B. Tomson and W. Chen, *Environ. Sci. Technol.*, 2012, **46**, 5422–5429.
25 Y. Wang, Y. Li, J. Costanza, L. M. Abriola and K. D. Pennell, *Environ. Sci. Technol.*, 2012, **46**, 11761–11769.
26 G. V. Andrievsky, M. V. Kosevich, O. M. Vovk, V. S. Shelkovsky and L. A. Vashchenko, *J. Chem. Soc., Chem. Commun.*, 1995, **12**, 1281–1282.
27 S. R. Chae, Y. Xiao, S. Lin, T. Noeiaghaei, J. O. Kim and M. R. Wiesner, *Water Res.*, 2012, **46**, 4053–4062.
28 X. Chang, L. K. Duncan, J. Jinschek and P. J. Vikesland, *Langmuir*, 2012, **28**, 7622–7630.
29 G. V. Andrievsky, V. K. Klochkov, A. B. Bordyuh and G. I. Dovbeshko, *Chem. Phys. Lett.*, 2002, **364**, 8–17.
30 K. L. Chen and M. Elimelech, *J. Colloid Interface Sci.*, 2007, **309**, 126–134.
31 H. Mashayekhi, S. Ghosh, P. Du and B. Xing, *J. Colloid Interface Sci.*, 2012, **374**, 111–117.
32 A. Franchi and C. R. O'Melia, *Environ. Sci. Technol.*, 2003, **37**, 1122–1129.
33 K. L. Chen and M. Elimelech, *Environ. Sci. Technol.*, 2008, **42**, 7607–7614.
34 T. Kanti Sen and K. C. Khilar, *Adv. Colloid Interface Sci.*, 2006, **119**, 71–96.
35 M. V. Avdeev, A. A. Khokhryakov, T. V. Tropin, G. V. Andrievsky, V. K. Klochkov, L. I. Derevyanchenko, L. Rosta, V. M. Garamus, V. B. Priezzhev, M. V. Korobov and V. L. Aksenov, *Langmuir*, 2004, **20**, 4363–4368.
36 K. Yang and B. Xing, *Environ. Pollut.*, 2007, **145**, 529–537.
37 P. Grathwohl, *Diffusion in Natural Porous Media: Contaminant Transport, Sorption/Desorption and Dissolution Kinetics*, Kluwer Academic, Norwell MA, 1997.